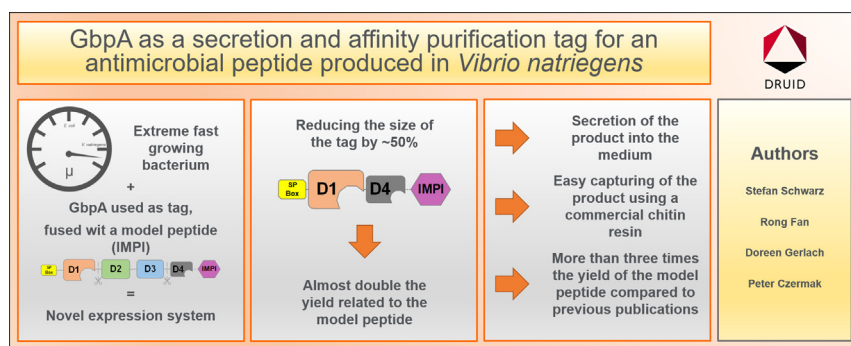




## Research Article

GbpA as a secretion and affinity purification tag for an antimicrobial peptide produced in *Vibrio natriegens*Stefan Schwarz<sup>a</sup>, Doreen Gerlach<sup>b</sup>, Rong Fan<sup>a,b</sup>, Peter Czermak<sup>a,c,\*</sup><sup>a</sup> Institute of Bioprocess Engineering and Pharmaceutical Technology, University of Applied Sciences Mittelhessen, Germany<sup>b</sup> Fraunhofer Institute for Molecular Biology and Applied Ecology, Branch for Bioresources, Germany<sup>c</sup> Faculty of Biology and Chemistry, Justus-Liebig-University Giessen, Germany

## GRAPHICAL ABSTRACT



## ARTICLE INFO

## Article history:

Received 12 July 2021

Accepted 26 January 2022

Available online 2 February 2022

## Keywords:

Affinity purification tag

Affinity tag

AMP

Antimicrobial peptide

GbpA

IMPI

Protein secretion

Recombinant

Secretion

Secretion purification tag

*Vibrio natriegens*

## ABSTRACT

**Background:** *Vibrio natriegens* is a Gram-negative bacterium that offers a greater metabolic capacity than *Escherichia coli* for the production of recombinant proteins. This potential includes a low minimum doubling time of 7 min and a high maximum glucose uptake rate of  $3.9 \text{ g} \cdot \text{g}^{-1} \cdot \text{h}^{-1}$ . We therefore tested the ability of *V. natriegens* to produce the insect metalloprotease inhibitor (IMPI), an antimicrobial peptide, fused to the glucosamine-binding protein A (GbpA) secretion/purification tag, using the Vmax Express system.

**Results:** The IMPI-GbpA fusion protein was secreted into the medium and could be purified directly from the fermentation supernatant by affinity chromatography, including on-column digestion with thrombin. We also modified the GbpA tag by deleting the second and third domains, which reduced the size of the tag while maintaining its functionality. This modification also increased the IMPI yield.

**Conclusions:** The use of *V. natriegens* as an expression platform and GbpA for protein secretion and purification facilitates the inexpensive production of antimicrobial peptides. Our process achieved a higher volumetric yield than earlier attempts to produce recombinant IMPI in *E. coli*. However, the accumulation of IMPI causes *V. natriegens* growth arrest before the carbon source is depleted, suggesting it may be possible to achieve even greater productivity by further process optimization.

**How to cite:** Schwarz S, Gerlach D, Fan R, et al. GbpA as a secretion and affinity purification tag for an antimicrobial peptide produced in *Vibrio natriegens*. Electron J Biotechnol 2022;56. <https://doi.org/10.1016/j.ejbt.2022.01.003>.

© 2022 Universidad Católica de Valparaíso. Production and hosting by Elsevier B.V. This is an open access article under the CC BY-NC-ND license (<http://creativecommons.org/licenses/by-nc-nd/4.0/>).

Peer review under responsibility of Pontificia Universidad Católica de Valparaíso

\* Corresponding author.

E-mail addresses: [peter.czermak@lse.thm.de](mailto:peter.czermak@lse.thm.de), [stefan.schwarz@lse.thm.de](mailto:stefan.schwarz@lse.thm.de) (P. Czermak).<https://doi.org/10.1016/j.ejbt.2022.01.003>

0717-3458/© 2022 Universidad Católica de Valparaíso. Production and hosting by Elsevier B.V.

This is an open access article under the CC BY-NC-ND license (<http://creativecommons.org/licenses/by-nc-nd/4.0/>).

## 1. Introduction

*Vibrio natriegens* is a halophilic, rod-shaped, Gram-negative bacterium [1] originally isolated from a salt marsh and classified as *Pseudomonas natriegens* [2,3]. It has a low minimum doubling time of 7 min [4,5] and a high glucose uptake rate of  $3.90 \text{ g} \cdot \text{g}^{-1} \cdot \text{h}^{-1}$ , making it suitable as a host platform for the production of recombinant proteins [6]. *V. natriegens* has already been used to express multiple variants of green fluorescent protein [7,8], membrane proteins from *Vibrio cholera* [9], and the FK506-binding protein for isotope labeling [10]. Furthermore, the enzyme uricase, the antimicrobial peptide (AMP) lucimycin and the insect metalloprotease inhibitor (IMPI) have been secreted into the *V. natriegens* periplasm using the ssYahJ tag [11]. *V. natriegens* has also been used for metabolic engineering [12]. Most recently, 149 different genes from bacteria, yeast, and plants were expressed in *V. natriegens* using pET vectors [13]. However, it has not yet been possible to secrete recombinant proteins produced by *V. natriegens* directly into the medium.

The secretion of recombinant proteins helps to prevent protein aggregation (in many cases by ensuring efficient folding and the formation of disulfide bonds), reduces the effect of toxic proteins on the host, and allows the direct capture of proteins from the medium, thus avoiding the need for bacterial lysis [14]. Among the six secretion systems known in Gram-negative bacteria, only the type II secretion system (T2SS) spans the inner and outer membranes and exports products in two steps, allowing folding and disulfide bond formation in the periplasm before secretion to the medium [15]. It is unclear how proteins in the periplasm are recognized and translocated through the outer membrane. The T2SS consists of 12–15 different proteins with the prefix Gsp (general secretion pathway) but the detailed assembly is not fully understood [16]. The substrates of this secretion system include cellulases, toxins and glucosamine-binding protein A (GbpA) [17,18].

The 54-kDa matrix protein GbpA has four domains that allow *V. cholerae* and related species to attach to chitinous and mucin-rich surfaces [19]. Domain I is related to the chitin-binding domain of *Serratia marcescens*, featuring two disulfide bonds and an N-terminal secretion sequence for translocation to the periplasm. Domains II and III resemble the S fimbriae periplasmic chaperone from *E. coli* and are required to bind the cell surface. Domain IV is similar to the chitin-binding domain of *S. marcescens* chitinase B [20]. Although GbpA is secreted via the T2SS, it lacks a Tat consensus sequence and probably uses the Sec pathway, as suggested by the bioinformatics tools Philius, Phobius, and SignalP [21,22,23]. In binding studies, more than 95% of GbpA binds to both chitin and *N*-acetylglucosamine (GlcNAc) beads, suggesting the protein could be suitable as a tag for affinity chromatography [20]. In this method, samples are applied to a column containing an immobilized affinity ligand, which retains the target for purification while other components elute in the wash buffer. The target is then released by eluting under conditions that cause the ligand and target to dissociate [24]. For fusion proteins, an elegant solution is to separate the affinity tag from the fusion partner by on-column enzymatic digestion, which can be achieved by placing a protease cleavage site between the fusion partners [25].

We elected to use *V. natriegens* combined with a GbpA fusion tag for the production of the insect metalloproteinase inhibitor (IMPI), the first specific metalloproteinase inhibitor from invertebrates, which was discovered in the greater wax moth *Galleria mellonella* [26]. IMPI is a cysteine-rich, trypsin inhibitor-like protease inhibitor (family I8), and is 69 amino acids in length with a molecular mass of 7.7 kDa (8.4 kDa including the *N*-linked glycans, which are not essential for activity) [26,27]. IMPI is thermotolerant and

functions at low pH due to the presence of five disulfide bridges [27]. It specifically inhibits M4-type metalloproteases such as aureolysin, pseudolysin and bacillolysin [28] and shows particularly low  $\text{IC}_{50}$  values against bacillolysin, pseudolysin and vibriolysin [29]. This makes IMPI a candidate for the therapeutic inhibition of microbial metalloproteases [30]. The testing of recombinant IMPI fused to glutathione *S*-transferase (GST) in a porcine skin wound model confirmed its potential for the treatment of wounds infected with *Pseudomonas aeruginosa* [28]. Soluble IMPI has been produced in *E. coli* but with low yields of 2.2 mg/L, even in a fed-batch process with a final  $\text{OD}_{600}$  of 127.5, partly reflecting the stagnation of cell growth [31]. IMPI has also been produced as insoluble inclusion bodies in *E. coli* [32]. We anticipated that the growth-limiting effects of IMPI could be avoided by secreting the product into the medium, and therefore selected the GbpA fusion tag for use in *V. natriegens*, allowing subsequent purification by affinity chromatography and on-column enzymatic digestion.

## 2. Methods

### 2.1. Cloning

The GbpA gene including the stop codon was amplified by PCR using Q5 Polymerase (New England Biolabs, Germany). The expression cassette, containing the GbpA and IMPI sequences separated by a thrombin cleavage site, was inserted into vector pAGM6413 using a two-step Golden Gate reaction [33,34]. The final vector (named GbpA 1) contained the expression cassette flanked by T7 promoter and terminator sequences as well as a spectinomycin-resistance gene to maintain selection pressure. A derivative vector (GbpA 2) was created by removing the GbpA stop codon, and a further derivative vector (GbpA 4) was created by removing domains II and III from the GbpA sequence.

### 2.2. Cultivation

We transformed *V. natriegens* with each of the three vectors and cultivated the transformants in triplicate, with induction after 2 h as described below. An additional culture containing GbpA 4 was cultivated without induction. Cells were cultivated in 1-L baffled shake flasks (Schott, Germany) at 250 rpm and 37°C in a Multitron shaking incubator (Infors, Germany). The flasks were filled with 100 mL modified M9 medium (Table S1) supplemented with 200 µg/mL spectinomycin (Sigma Aldrich, USA) and 5 g/L glucose (Carl Roth, Germany). The pre-warmed shaking flasks were inoculated by adding 1 mL of a cryo-preserved *V. natriegens* 20% glycerol stock ( $\text{OD}_{600} = 10$ ). After a 140 min growth phase, IMPI production was induced by adding IPTG (Carl Roth) to a final concentration of 50 µM.

### 2.3. Sampling strategy

Samples (1.5 mL) were taken at  $t = 0$  (inoculation), every hour from inoculation to induction, immediately after induction, and every hour from induction to harvest. From each sample, 1 mL was centrifuged at  $16,000 \times g$  for 5 min at 4°C, and the pellets and supernatant (300-µL aliquots) were individually frozen at –20°C in for subsequent analysis. The remaining 500 µL of the original sample was used to determine the pH and  $\text{OD}_{600}$ , and to measure the glucose concentration in a BIOSEN C-line (EKF-diagnostic, Germany).

## 2.4. Harvest

The culture broth was harvested 7 h post-induction. From each flask, 70 mL of broth was divided into two equal portions in 50-mL Falcon tubes, which were centrifuged at  $15,000 \times g$  for 5 min at 4°C. The supernatant was separated from the pellet and frozen at –20°C. One of two pellets per flask was cryo-preserved and the other was resuspended in 40 mL phosphate-buffered saline (PBS) and centrifuged again. The pellet was then dried at 65°C for 48 h to determine the cell dry weight.

## 2.5. Affinity chromatography

Two Pierce 10-mL centrifuge columns (Thermo Fisher Scientific, USA) were filled with 1 mL chitin resin in storage buffer (New England Biolabs) and the buffer was removed by centrifugation at  $700 \times g$  for 3 min at 25°C. The columns were equilibrated by washing three times with 10 mL wash and binding buffer (WB) consisting of 150 mM NaCl, 50 mM Tris and 2.5 mM CaCl<sub>2</sub> (pH 8.0). The columns were loaded with 10 mL supernatant harvested from the GbpA 2 and GbpA 4 cultures, respectively. The columns were incubated for 1 h on a Revolver rotating platform (Labnet, USA) then centrifuged as above and the fractions were collected (1 mL of each fraction was frozen at –20°C for SDS-PAGE analysis). The columns were washed with 10 mL WB and centrifuged as above, and this step was carried out three times in total. Each column was then loaded with 1 mL WB supplemented with 30 units of thrombin (Merck, Germany) and incubated at room temperature for 20 h on the rotating platform. The columns were centrifuged as above to elute the released IMPI, and any residual IMPI was eluted in two subsequent wash steps with 1 mL WB as described above. The columns were regenerated by incubation in 10 mL WB supplemented with 1% SDS for 30 min on the rotating platform before removing the regeneration buffer by centrifugation as above and repeating the step with regeneration buffer and water.

## 3. Analytics

### 3.1. SDS-PAGE and western blot

Cell pellets from the culture samples were disrupted by chemical and enzymatic lysis with 0.7 mL BugBuster Mastermix according to the manufacturer's protocol. The resulting insoluble and soluble fractions were mixed 3:1 with Laemmli mix, consisting of a 9:1 ratio of 4 × Laemmli buffer and 2-mercaptoethanol (both from Bio-Rad, USA). The mixed samples were denatured at 98°C for 10 min. We then loaded 13-μL sample aliquots alongside 3 μL Bio-Rad protein markers onto the gel, which was placed in a Criterion Cell (Bio-Rad) filled with TGS buffer (Bio-Rad). The proteins were separated at 250 V for 25 min using a PowerPac Basic power supply (Bio-Rad). Gel images were analyzed using the ChemiDoc MP Imaging System and Image Lab software (Bio-Rad).

For western blot analysis, proteins were transferred from the gel to a PVDF membrane (Bio-Rad) using the Trans-Blot Turbo system (Bio-Rad). The membrane was blocked for 1 h in 5 g/L bovine serum albumin (BSA) in PBS containing 0.05% Tween-20, then washed three times for 5 min in PBS containing 0.1% Tween-20 (PBST). The membrane was then incubated with 15 mL of the custom primary antibody solution (Eurogentec, Belgium) with an antibody concentration of 2 mg/L. After three further wash steps as above, the membrane was incubated overnight in 15 mL of the secondary antibody solution comprising 0.16 mg/L goat anti-rabbit IgG (Thermo Fisher Scientific) and 1.5 μL StrepTactin-HRP Conjugate (Bio-Rad). After three further washes, the membrane was

overlaid with 5 mL of the Clarity Western ECL Substrate (Bio-Rad) for 3 min before visualization.

### 3.2. Determination of the product concentration

A 10 g/L suspension of chitin (Sigma-Aldrich) in water (35 mL in a 50-mL Falcon tube) was centrifuged at  $5000 \times g$  for 5 min at room temperature and the pellet was resuspended in the same volume of water and kept in suspension by continuous stirring. We then dispensed 0.4-mL aliquots to 1.5-mL tubes and evaporated the water in a dry cabinet at 65°C overnight. The dry chitin aliquots were stored at room temperature.

Bradford solution was prepared as previously described [35]. The cell-free culture supernatant was then divided into two fractions, 100 μL of which was retained and 200 μL was transferred to a dry chitin aliquot. The supernatant mixed with the chitin aliquot was shaken at 1000 rpm at 25°C in a Thermomixer Comfort (Eppendorf, Germany) for 30 min. The aliquots were centrifuged at  $16,000 \times g$  for 5 min, and the supernatant (130 μL) was transferred to a fresh tube.

The Bradford assay was carried out in 96-well plates (Greiner Bio-One International, Austria) in triplicate, including blank and calibration values. The blank was water. The assay was calibrated in eight equidistant steps from 7.5 to 60 mg/L. The standard was BSA fraction V (Carl Roth). We transferred 30 μL of each sample per well and added 270 μL of the Bradford solution. Absorption at 450 and 595 nm was measured using a Synergy HT plate reader (BioTek Instruments, USA) and Gen5 software. The protein concentration was calculated from the quotient of the two absorption values [36]. The product concentration was determined by calculating the difference between the protein concentrations before and after incubation of the culture supernatant with chitin. The assay required a product concentration of 15–35 mg/L and samples in excess of the maximum value were therefore diluted in PBS.

To calculate the concentration of IMPI from the fusion protein concentration, we used the online tool ProtParam from ExPASy. With this tool we determined the weight fraction of IMPI in the fusion protein and thus concluded the concentration of IMPI. We did the same with the data from the processes used to compare the product concentrations.

All *t*-tests in this publication were performed in OriginPro software from OriginLab Corporation, using software version 9.0.0.

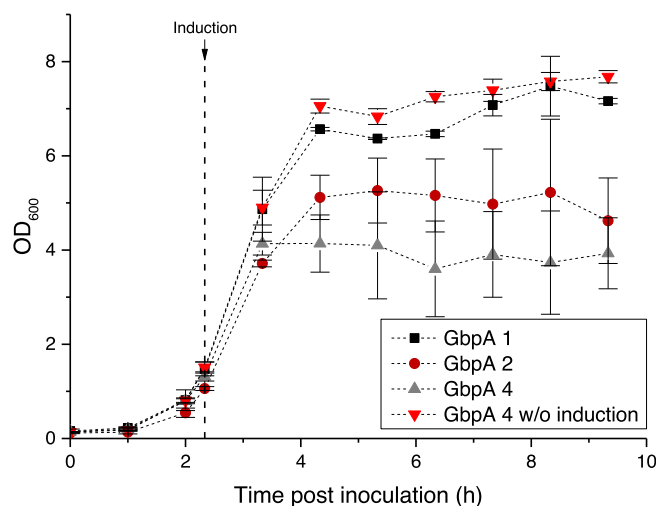


**Fig. 1.** Measurement of cell density (OD<sub>600</sub>) in shaking flasks containing *V. natriegens* transformed with constructs GbpA 1, GbpA 2 or GbpA 4 (the latter with and without induction). Data are means ± SD (*n* = 3).

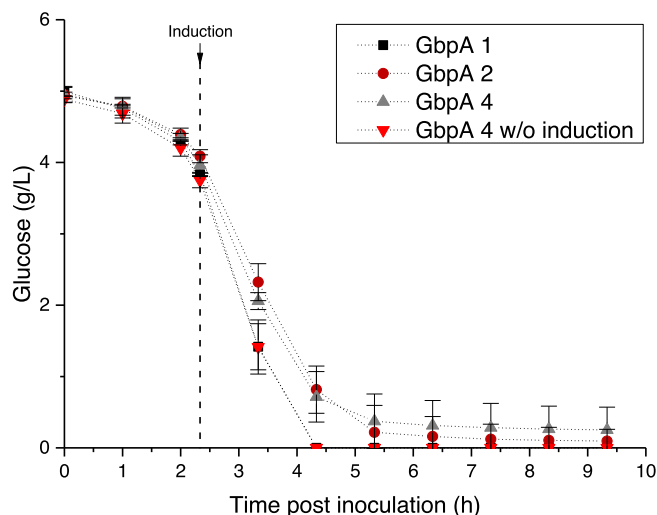


**Fig. 2.** Measurement of glucose levels in shaking flasks containing *V. natriegens* transformed with constructs GbpA 1, GbpA 2 or GbpA 4 (the latter with and without induction). Data are means  $\pm$  SD ( $n = 3$ ).

#### 4. Results

We initiated two *V. natriegens* cultures for the induction of the fusion protein GbpA-IMPI, one with a full-length construct (GbpA 2) and the other with domains II and III removed from the fusion tag (GbpA 4). We also initiated two control cultures, one (GbpA 1) induced to produce the GbpA tag alone, which was achieved by leaving the stop codon in place after the GbpA sequence, and the other was GbpA 4 without induction. The growth curves of all four cultures were generally similar (Fig. 1). However, the post-induction OD<sub>600</sub> values were lower for the IMPI-producing cultures (GbpA 2 and GbpA 4) and the variation around the mean was also greater, as shown by the larger error bars (Fig. 1). This reflected the formation of cell aggregates in these cultures, which were visible to the naked eye as a more turbid fermentation broth.

The glucose consumption profiles (Fig. 2) of the four cultures also fell into two categories. For the control experiments (GbpA 1 and GbpA 4 without induction), the glucose was completely depleted 2 h post-induction. In contrast, IMPI expression (GbpA 2

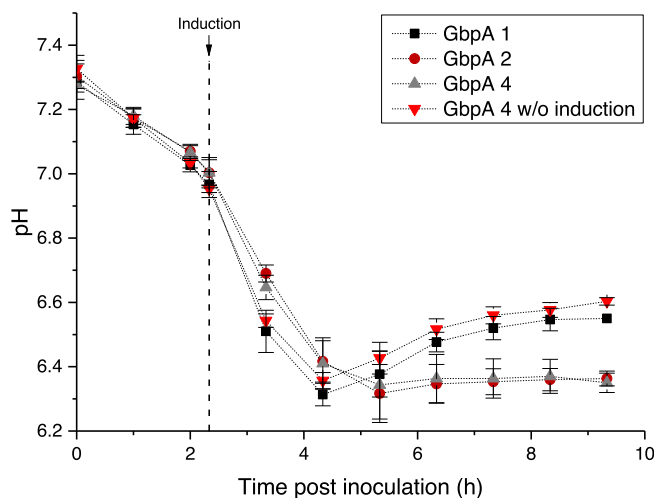


**Fig. 3.** Measurement the pH of the medium in shaking flasks containing *V. natriegens* transformed with constructs GbpA 1, GbpA 2 or GbpA 4 (the latter with and without induction). Data are means  $\pm$  SD ( $n = 3$ ).

and GbpA 4) caused the slower consumption of glucose, with some of the substrate still remaining 7 h post-induction.

Likewise, the pH profiles differed between the control experiments and IMPI production (Fig. 3). In the control experiments, the pH steadily declined until  $\sim 2$  h post-induction and then began to climb again, whereas the pH decline continued until  $\sim 3$  h post-induction in the IMPI production experiments and then reached a plateau at pH  $\sim 6.3$ .

The comparison of dry cell masses also showed higher values for the control cultures compared to those producing IMPI, and the non-induced culture also accumulated significantly more biomass than the GbpA 1 culture producing free fusion tag (Fig. 4).

The OD<sub>600</sub> values and dry masses were compared to establish correlations, which were then used to calculate substrate-specific biomass yield coefficients in the period from inoculation to 260 min post-inoculation (Fig. 5). The glycerol introduced from the cryo-preservation medium was ignored. Interestingly, we observed no significant difference between GbpA 1 (fusion tag alone) and GbpA 2 (complete GbpA-IMPI fusion construct), but a

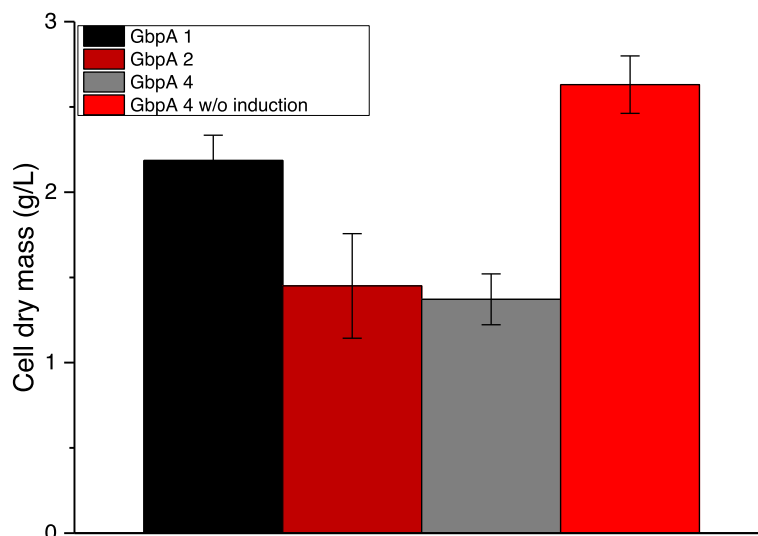


**Fig. 4.** Cell dry mass at the time of harvest in shaking flasks containing *V. natriegens* transformed with constructs GbpA 1, GbpA 2 or GbpA 4 (the latter with and without induction). Data are means  $\pm$  SD ( $n = 3$ ). All values are significantly different from each other ( $t$ -test,  $p < 0.05$ ) except GbpA 2 vs GbpA 4.

significantly lower value for GbpA 4 (GbpA-IMPI fusion construct lacking domains II and III) and a significantly higher value for the non-induced GbpA 4.

Samples collected during fermentation were centrifuged to separate the cells from the medium and the cells were lysed to yield soluble and insoluble fractions for comparative analysis by SDS-PAGE (Fig. 6). A 50-kDa band representing the GbpA tag without a fusion partner (GbpA 1) appeared 1 h post-induction, whereas the 58-kDa GbpA-IMPI fusion protein (GbpA 2) and its shorter derivative (GbpA 4, 32 kDa) took longer to accumulate, first becoming visible 2 h post-induction. Distribution between the soluble and insoluble fractions also differed depending on the product, with a greater proportion of the lone GbpA tag appearing in the soluble fraction compared to the IMPI fusion proteins. A comparison of GbpA 2 and GbpA 4, which differ solely in the domain structure of the GbpA tag, showed that the GbpA 4 product (32 kDa) was less abundant than GbpA 2 (~58-kDa) in the soluble fraction after cell lysis in samples recovered 3 h post-induction and later. GbpA 4

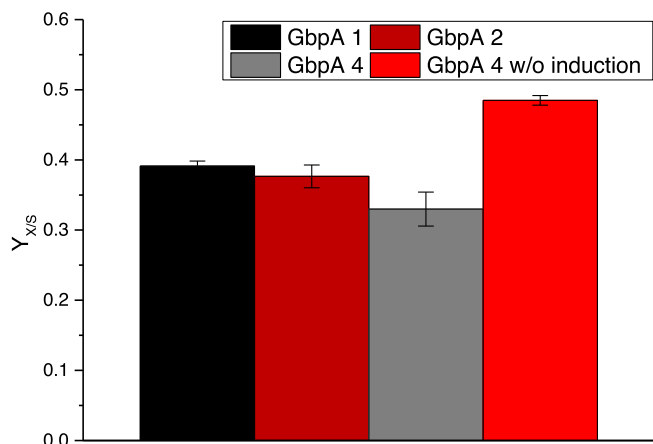


**Fig. 5.** Substrate-specific biomass yield coefficients calculated for the first 260 min of cultivations in shaking flasks containing *V. natriegens* transformed with constructs GbpA 1, GbpA 2 or GbpA 4 (the latter with and without induction). Data are means  $\pm$  SD ( $n = 3$ ). All values are significantly different from each other ( $t$ -test,  $p < 0.05$ ) except GbpA 1 vs GbpA 2.

also featured an extra 37-kDa band in the insoluble fraction that first became visible 1 h post-induction.

Product quantification in the cell-free supernatant revealed that the free GbpA tag (GbpA 1) accumulated to significantly higher levels than the fusion proteins, but there was no significant difference between the full-length fusion (GbpA 2) and the shorter version (GbpA 4) lacking domains II and III (Fig. 7).

The GbpA 2 and GbpA 4 products were purified from the culture supernatant by affinity chromatography (Fig. 8). In both cases, a dominant product band was observed in the loading lane alongside a weak corresponding band in the flow-through lane, with the anticipated sizes of 58 kDa (GbpA 2) and 32 kDa (GbpA 4). The released IMPI product was not visible in the SDS-PAGE elution lanes because it lacks tryptophan, which is the amino acid bound by the protein stain. The band that is visible in the SDS-PAGE elution lanes corresponds to the anticipated size of thrombin, the cleavage enzyme (~30 kDa). However, the released IMPI product was detected by western blot with the anticipated size of ~7.7 kDa. Given the much stronger signal in the GbpA 4 blot, the recovery of IMPI was more efficient when initially fused to the shorter GbpA tag lacking domains II and III. Most of the product was recovered in the first elution fraction, and in the case of GbpA 4, the remainder was recovered in the second elution fraction, with none appearing in the third elution fraction. The regeneration lanes confirmed the release of the cleaved GbpA tag, with no corresponding signal in the western blot.

## 5. Discussion

The production of IMPI as a therapeutic candidate has been hampered by its impact on the growth of *E. coli*, resulting in low yields of 2.2 mg/L in a fed-batch process with a final OD<sub>600</sub> of 127.5 [31]. We hypothesized that the growth-limiting effects of IMPI probably reflect interactions with intracellular targets and should be avoided by secreting the product into the medium, which also provides a more straightforward strategy for product purification [14]. We therefore selected *V. natriegens* as a production host with IMPI expressed as a GbpA fusion to facilitate both secretion and recovery by affinity chromatography on a chitin-based resin. Expression of the fusion protein was induced by the addition of IPTG to *V. natriegens* cultures in shake flasks, and as

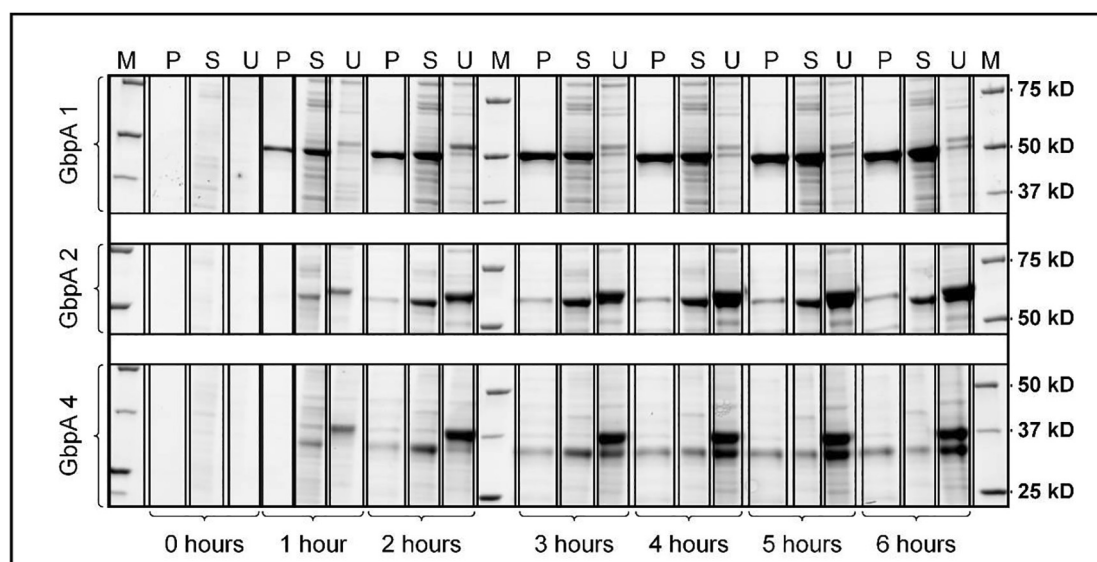


**Fig. 6.** SDS-PAGE analysis of cultivation samples from induction until 1 h before harvest. M = marker, P = cell-free supernatant, S = soluble fraction after cell lysis, U = insoluble fraction after cell lysis.

controls we used the induction of the lone GbpA tag and a non-induced culture of the fusion protein, enabling us to separately test the effect of induction and the presence of the IMPI polypeptide on *V. natriegens* growth and productivity.

We found that the control cultures achieved higher OD<sub>600</sub> values than the cultures expressing IMPI fusion proteins, and that the latter also tended to aggregate resulting in more variable OD<sub>600</sub> readings (Fig. 1). The IMPI cultures also accumulated significantly less cell dry mass (Fig. 4). To ensure the data were meaning-

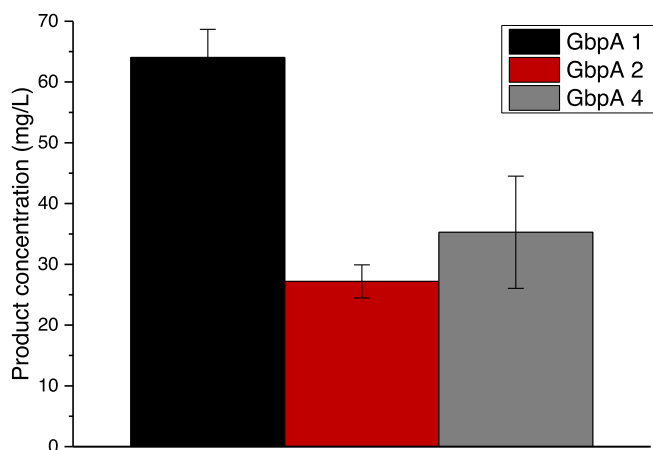


**Fig. 7.** Product concentrations in the cell-free supernatant at the point of harvest for shaking-flask cultures containing *V. natriegens* transformed with constructs GbpA 1, GbpA 2 or GbpA 4. Data are means  $\pm$  SD ( $n = 3$ ). All values are significantly different from each other ( $t$ -test,  $p < 0.05$ ) except GbpA 2 vs GbpA 4.

ful, we calculated the quotient of OD<sub>600</sub> and cell dry mass, resulting in values of  $3.28 \pm 0.12$  (GbpA 1),  $3.21 \pm 0.08$  (GbpA 2),  $2.86 \pm 0.23$  (GbpA 4) and  $2.92 \pm 0.08$  (GbpA 4 without induction). These values did not differ significantly between the control cultures and those producing IMPI ( $t$ -test,  $p \geq 0.05$ ) suggesting that the OD<sub>600</sub> data are indeed meaningful in the context of cell dry mass. Cell aggregation can be triggered by multiple stimuli, including changes in temperature, oxygen availability or stress, but only cells expressing IMPI were affected in our experiments, suggesting that IMPI accumulation is stressful to the cells [37].

The expression of IMPI fusion proteins led to growth arrest despite the presence of non-depleted substrate, as previously observed in *E. coli* [31]. However, we also observed significantly lower substrate-specific biomass yields during IMPI production compared to the non-induced culture (Fig. 5). We assume that the falling pH (Fig. 3) reflects the accumulation of acids during aerobic cultivation, similar to the previously reported formation of 0.8 mol acetic acid per mol glucose [38]. After the glucose has been consumed, the acetic acid serves as a substrate, leading to the increase in pH observed in the case of GbpA 1 (starting 3 h post-induction) and in the GbpA 4 culture without induction. This leads to further growth, and presumably the glycerol introduced by the cryo-preservation medium is also consumed as a carbon source during this phase.

In studies with other Gram-negative bacteria, it was shown that centrifugation forces of more than  $5,000 \times g$  can lead to cell surface damage [39]. For this reason, it could have been that the product secreted into the supernatant was a result of damage to the cell surface. To rule this out, comparative experiments were performed at  $5,000 \times g$  and  $15,000 \times g$  during cell harvest. The results exclude such an effect and are deposited in Figure S1, Figure S2 and Table S2.

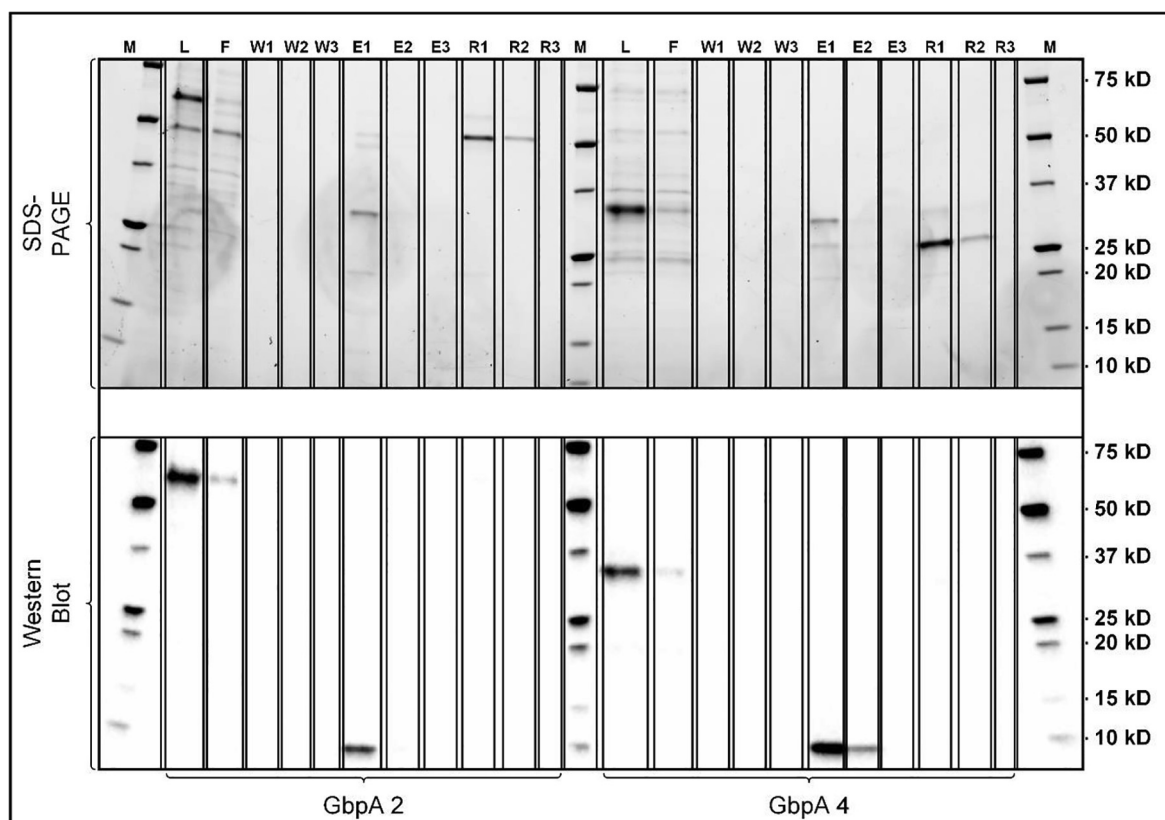


**Fig. 8.** SDS-PAGE and western blot analysis of GbpA 2 and GbpA 4 samples before and during affinity chromatography. M = marker, L = load, F = flow-through, W = wash, E = elution, R = resin regeneration. The volume of all fractions was 10 mL except the elution fractions (1 mL).

The difference in product concentrations between GbpA 2 and GbpA 4 was not significant (Fig. 7), but when the proportion of IMPI in the product is considered there is a clear increase in IMPI yield due to the smaller size of the GbpA 4 tag. In the case of GbpA 2, the proportion is ~13%, but this rises to ~24% for GbpA 4, representing a two-fold increase in yield for the same fusion protein concentration. The GbpA 1 culture also produced approximately twice as much product as GbpA 2 or GbpA 4 as well as significantly more biomass, suggesting that IMPI expression places a heavy burden on bacterial metabolism but the productivity limits of the production platform have yet to be reached. Nevertheless, we achieved yields of soluble IMPI far exceeding previous reports. Given a fusion protein yield of 35.3 mg/L for GbpA 4, our IMPI yield was ~8.5 mg/L. The fusion product concentration previously reported in *E. coli* was 20.4 mg/L, and taking the size of IMPI and the elastin-like polypeptide (ELP) fusion partner into account this corresponds to an IMPI yield of ~2.2 mg/L [31]. The difference is even more pronounced for the biomass-specific yield of ~5.9 mg/g in our study and ~0.065 mg/g in *E. coli* [31]. A GST-IMPI fusion protein was expressed in *E. coli* with a yield of 5.73 mg/L, corresponding to an IMPI yield of ~1.27 mg/L [40]. However, the GST-IMPI fusion was expressed in cells growing in complex medium whereas chemically defined medium was used for the ELP fusion product.

SDS-PAGE analysis of the fermentation samples showed that the accumulation of product in the insoluble fractions can probably be attributed to IMPI (Fig. 6). IMPI produced in *E. coli* Rosetta-gami™ 2, a mutant that allows the formation of disulfide bridges in the cytoplasm, is completely insoluble without a fusion tag [40]. Comparing the band patterns of GbpA 2 and GbpA 4, we see that in the case of GbpA 4, there is a smaller amount of soluble product in the soluble fraction of the cell lysis compared to the product in the cell-free supernatant (Fig. 6). This may have two causes, which are not mutually exclusive. One possible cause is that the smaller tag could not be sufficient to keep IMPI in a solution state, resulting in a greater proportion remaining in the insoluble fraction of the cell lysis. The mechanisms by which protein tags increase the solubility of their fusion partners are not fully understood, and several hypotheses exist. One of these hypotheses is that fusion partners may have intrinsic chaperone-like activity. In this case, hydrophobic regions on the tag interact with the partially folded fusion partner, preventing aggregation of the target protein. Another hypothesis is that strongly acidic tags prevent aggregation by electrostatic repulsion [41]. Consistent with the last theory, most tags used to improve solubility have a PI of 4 to 5 and a GRAVY (grand average of hydropathicity) of about 0 to -1. The GRAVY circumscribes the hydrophobicity/hydrophilicity of a protein, the more negative this value, the more hydrophilic the protein [42]. Both theories represent possible explanations for a possible lower solubility-mediating effect of the GbpA 4 tag. Removal of two domains increases the theoretical isoelectric point of the tag from 4.95 to 5.58, but the GRAVY changes only slightly from -0.509 to -0.483, making the tag more hydrophilic (both values were determined using the ProtParam tool from ExPASy). However, because the GRAVY is only a relative value with respect to the total number of amino acids, it cannot be excluded that no relevant hydrophobic regions were removed by the loss of domains II and III.

Another cause is that GbpA binds partially to the cell surface, and may be separated when the cells are removed from the medium. This co-separated fusion protein would then be found in the fractions of the cell lysis. Depending on how the binding of the fusion protein to cell surface components behaves after cell lysis, this portion of the fusion protein may be found in both the soluble and insoluble fractions of the cell disruption. We assume that this effect is suppressed when domains II and III are removed. These

domains interact with the cell surface. For this reason, in the case of GbpA 4, less soluble protein is separated from the supernatant along with the cells because it is not present bound to the cell surface, which ensures that in the case of GbpA 4, it appears that more soluble fusion protein is present in the cell compared to the soluble fusion protein in the cell-free supernatant. The hypothesis that secreted GbpA proteins and adhesins are partly in solution and partly bound on the cell surface has been explored for *V. cholerae* [43,44]. If both hypotheses are correct, the product titer could be increased by deleting either domain II or domain III but not both. In this scenario, the deletion of one domain must restrict the binding of the fusion protein to the cell surface and the other domain must increase the solubility of the fusion protein in the cell.

SDS-PAGE also revealed a double band in the GbpA 4 lane for the insoluble fraction after cell lysis (32 and 37 kDa) starting 3 h post-induction. The most likely explanation is the separation of the secretion signal during the translocation of the fusion protein via the Sec pathway into the periplasm. This is consistent with the identification of the first 23 amino acids of the GbpA sequence as the secretion signal for the Sec pathway using three bioinformatics tools: Philius, Phobius, and SignalP 5.0 [21,22,23]. This is also supported by the time delay, with the 37-kDa band already detected 1 h post-induction and the weaker 32-kDa band another hour later. This is logical if one considers that the protein is translated into the cytoplasm and can only accumulate in the periplasm without the signal sequence following transport via the inner membrane. On closer inspection, the same effect is present in the GbpA 1 and GbpA 2 gels. Looking at the product bands present in the soluble and insoluble fractions of the lysed cells 1 h post-induction, the product band in the insoluble fraction is slightly above than the product band in the soluble fraction in all cases, reflecting the time delay caused by transport across the inner membrane. Also very well observed in the case of GbpA 2 and GbpA 4 is the time delay of one hour between the appearance of the product band in the soluble fraction of the cell lysis and its appearance in the cell-free supernatant. We assume that this can be explained by the previously described sequence of secretion via the T2SS. After the protein to be secreted has first been transported into the periplasm, it is secreted into the surrounding medium by the T2SS machinery in the next step. Strikingly, the last delay is observed only for the IMPI-containing fusion proteins. Thus, the second delay appears to be increased by fusion with IMPI.

During affinity purification, a small amount of the fusion protein did not bind to the resin and thus appeared as a weak band in the flow-through (Fig. 8), probably due to partial inactivation caused by freezing and thawing of the supernatant. Overloading of the resin can be excluded because a similar distribution of bands between the loading and the flow-through lanes was observed in an identical experiment with double loading of the resin (data not shown). In the regeneration fractions, only the tag band is seen in the SDS-PAGE lanes, suggesting that 20 h was sufficient for complete thrombin digestion. The purification and simultaneous concentration of IMPI can therefore be considered successful. Given that a small part of the tag was inactivated by freezing and thawing, we also assume that product concentrations in the supernatant are lower than the actual concentrations because the assay that measures product concentrations is based on the separation of the product by binding to chitin.

We currently lack a satisfactory elution strategy without inducing tag denaturation. However, initial experiments have shown that the binding of the tag is extremely stable over a wide pH range of 2–11 in phosphate buffer with a concentration of 0.3–0.4 M. Even 0.1 M HCl did not elute the tag from chitin. The tag also remains stable at temperatures up to at least 60°C (data not shown). This opens up possibilities for the immobilization of enzymes and other fusion proteins, as already demonstrated at

60°C with another chitin-binding domain [45]. Another promising approach is elution with acetic acid as reported for the chitin-binding domain of *Bacillus circulans* [46] which we are currently adapting for the GbpA tag. The strong bond between the tag and its ligand is both beneficial and a drawback, because it has created a defined interface between upstream and downstream processing. Following the secretion of the product, the fusion protein can be bound directly to the resin after cell separation without cell disruption and re-buffering. For further optimization of this interface, we will explore the possibility of cell separation using membranes to achieve the more economical and scalable separation of recombinant protein products from host cells.

## Financial support

We thank the Hessen State Ministry of Higher Education, Research and the Arts for the financial support within the Hessen initiative for scientific economics excellence (LOEWE-Program and LOEWE Center DRUID (Novel Drug Targets against Poverty-Related and Neglected Tropical Infectious Diseases)).

## Conflict of interest

The authors declare that they have no known competing financial interests or personal relationships that could have appeared to influence the work reported in this paper.

## Acknowledgments

We thank Torsten Waldminghaus (Synmikro, Marburg, Germany) for providing the MoClo vectors and the genomic *V. cholerae* DNA, Joel Eichmann for help with the cloning, and Richard M. Twyman for professional editing of the manuscript.

## Supplementary material

<https://doi.org/10.1016/j.ejbt.2022.01.003>.

## References

- [1] Austin B, Zachary A, Colwell RR. Recognition of *Beneckea natriegens* (Payne et al.) Baumann et al. as a member of the Genus *Vibrio*, as previously proposed by Webb and Payne. *Int J Syst Bacteriol* 1978;28:315–7. <https://doi.org/10.1099/00207173-28-2-315>.
- [2] Payne WJ. Studies on bacterial utilization of uronic ACIDS III: Induction of Oxidative Enzymes in a Marine Isolate. *J Bacteriol* 1958;76:301–7. <https://doi.org/10.1128/JB.76.3.301-307.1958>. PMID: 13575389.
- [3] Payne WJ, Eagon RG, Williams AK. Some observations on the physiology of *Pseudomonas natriegens* nov. spec.. *Antonie Van Leeuwenhoek* 1961;27:121–8. <https://doi.org/10.1007/BF02538432>. PMID: 13733692.
- [4] Eagon RG. *Pseudomonas natriegens*, a marine bacterium with a generation time of less than 10 minutes. *J Bacteriol* 1962;83:736–7. PMID: 13888946.
- [5] Bianconi G, Fani R, Canganella F, et al. Draft Genome Sequence of the Fast-Growing Bacterium *Vibrio natriegens* Strain DSMZ 759. *Genome Announc* 2013;1:648–61. <https://doi.org/10.1128/genomea.00648-13>. PMID: 23969053.
- [6] Grenz S, Nitschel R, Müller F, et al. High substrate uptake rates empower *Vibrio natriegens* as production host for industrial biotechnology. *Appl Environ Microbiol* 2017;83. <https://doi.org/10.1128/AEM.01614-17>. PMID: 28887417.
- [7] Lee HH, Ostrov N, Wong BG, et al. Functional genomics of the rapidly replicating bacterium *Vibrio natriegens* by CRISPRi. *Nat Microbiol* 2019;4:1105–13. <https://doi.org/10.1038/s41564-019-0423-8>.
- [8] Weinstock MT, Hesk ED, Wilson CM, et al. *Vibrio natriegens* as a fast-growing host for molecular biology. *Nat Methods* 2016;13:849–51. <https://doi.org/10.1038/nmeth.3970>. PMID: 27571549.
- [9] Schleicher L, Muras V, Claussen B, et al. *Vibrio natriegens* as host for expression of multisubunit membrane protein complexes. *Front Microbiol* 2018;9:1–10. <https://doi.org/10.3389/fmicb.2018.02537>. PMID: 30410475.
- [10] Becker W, Wimberger F, Zangger K. *Vibrio natriegens*: an alternative expression system for the high-yield production of isotopically labeled proteins. *Biochemistry* 2019;58:2799–803. <https://doi.org/10.1021/acs.biochem.9b00403>. PMID: 31199119.
- [11] Eichmann J, Oberpaul M, Weidner T, et al. Selection of high producers from combinatorial libraries for the production of recombinant proteins in *Escherichia coli* and *Vibrio natriegens*. *Front Bioeng Biotechnol* 2019;7. <https://doi.org/10.3389/fbioe.2019.00254>.
- [12] Ellis GA, Tschirhart T, Spangler J, et al. Exploiting the feedstock flexibility of the synthetic biology chassis *Vibrio natriegens* for engineered natural product production. *Mar Drugs* 2019;17:1–21. <https://doi.org/10.3390/md17120679>. PMID: 31801279.
- [13] Xu J, Dong F, Wu M, et al. *Vibrio natriegens* as a pET-compatible expression host complementary to *Escherichia coli*. *Front Microbiol* 2021;12:1–11. <https://doi.org/10.3389/fmicb.2021.627181>. PMID: 33679648.
- [14] Freudl R. Signal peptides for recombinant protein secretion in bacterial expression systems. *Microb Cell Fact* 2018;17:52. <https://doi.org/10.1186/s12934-018-0901-3>. PMID: 29598818.
- [15] Costa TRD, Felisberto-Rodrigues C, Meir A, et al. Secretion systems in Gram-negative bacteria: Structural and mechanistic insights. *Nat Rev Microbiol* 2015;13:343–59. <https://doi.org/10.1038/nrmicro3456>. PMID: 25978706.
- [16] Korotkov KV, Sandkvist M, Hol WGJ. The type II secretion system: Biogenesis, molecular architecture and mechanism. *Nat Rev Microbiol* 2012;10:336–51. <https://doi.org/10.1038/nrmicro2762>. PMID: 22466878.
- [17] Burdette LA, Leach SA, Wong HT, et al. Developing Gram - negative bacteria for the secretion of heterologous proteins. *Microb Cell Fact* 2018;17. <https://doi.org/10.1186/s12934-018-1041-5>. PMID: 30572895.
- [18] Sikora AE, Zielke RA, Lawrence DA, et al. Proteomic analysis of the *Vibrio cholerae* type II secretome reveals new proteins, including three related serine proteases. *J Biol Chem* 2011;286:16555–66. <https://doi.org/10.1074/jbc.M110.211078>. PMID: 21385872.
- [19] Stauder M, Huq A, Pezzati E, et al. Role of GbpA protein, an important virulence-related colonization factor, for *Vibrio cholerae*'s survival in the aquatic environment. *Environ Microbiol Rep* 2012;4:439–45. <https://doi.org/10.1111/j.1758-2229.2012.00356.x>. PMID: 23760830.
- [20] Wong E, Vaaje-Kolstad G, Ghosh A, et al. The *Vibrio cholerae* colonization factor GbpA possesses a modular structure that governs binding to different host surfaces. *PLoS Pathog* 2012;8:e1002373. <https://doi.org/10.1371/journal.ppat.1002373>. PMID: 22253590.
- [21] Käll L, Krogh A, Sonnhammer ELL. Advantages of combined transmembrane topology and signal peptide prediction—the Phobius web server. *Nucleic Acids Res* 2007;35:429–32. <https://doi.org/10.1093/nar/gkm256>. PMID: 17483518.
- [22] Reynolds SM, Käll L, Riffle ME, et al. Transmembrane topology and signal peptide prediction using dynamic Bayesian networks. *PLoS Comput Biol* 2008;4:e1000213. <https://doi.org/10.1371/journal.pcbi.1000213>. PMID: 18989393.
- [23] Almagro Armenteros JJ, Tsirigos KD, Sønderby CK, et al. SignalP 5.0 improves signal peptide predictions using deep neural networks. *Nat Biotechnol* 2019;37:420–3. <https://doi.org/10.1038/s41587-019-0036-z>. PMID: 30778233.
- [24] Rodriguez EL, Poddar S, Iftekhar S, et al. Affinity chromatography: A review of trends and developments over the past 50 years. *J Chromatogr B* 2020;1157:. <https://doi.org/10.1016/j.jchromb.2020.122332>. PMID: 32871378122332.
- [25] Dian C, Eshaghi S, Urbig T, et al. Strategies for the purification and on-column cleavage of glutathione-S-transferase fusion target proteins. *J Chromatogr B* 2002;769:133–44. [https://doi.org/10.1016/S1570-0232\(01\)00637-7](https://doi.org/10.1016/S1570-0232(01)00637-7).
- [26] Wedde M, Weise C, Kopacek P, et al. Purification and characterization of an inducible metalloprotease inhibitor from the hemolymph of greater wax moth larvae, *Galleria mellonella*. *Eur J Biochem* 1998;255:535–43. <https://doi.org/10.1046/j.1432-1327.1998.2550535.x>.
- [27] Wedde M, Weise C, Nuck R, et al. The insect metalloproteinase inhibitor gene of the lepidopteran *Galleria mellonella* encodes two distinct inhibitors. *Biol Chem* 2007;388. <https://doi.org/10.1515/BC.2007.013>. PMID: 17214556.
- [28] Eisenhardt M, Schlupp P, Höfer F, et al. The therapeutic potential of the insect metalloproteinase inhibitor against infections caused by *Pseudomonas aeruginosa*. *J Pharm Pharmacol* 2019;71:316–28. <https://doi.org/10.1111/jphpp.13034>. PMID: 30408181.
- [29] Clermont A, Wedde M, Seitz V, et al. Cloning and expression of an inhibitor of microbial metalloproteinases from insects contributing to innate immunity. *Biochem J* 2004;382:315–22. <https://doi.org/10.1042/BJ20031923>. PMID: 15115439.
- [30] Vilcinskas A. ANTI-infective therapeutics from the lepidopteran model host *Galleria mellonella*. *Curr Pharm Des* 2011;17:1240–5. <https://doi.org/10.2174/138161211795703799>. PMID: 21470117.
- [31] Joachim M, Maguire N, Schäfer J, et al. Process intensification for an insect antimicrobial peptide elastin-like polypeptide fusion produced in redox-engineered *Escherichia coli*. *Front Bioeng Biotechnol* 2019;7. <https://doi.org/10.3389/fbioe.2019.00150>. PMID: 31316976.
- [32] Hoffmann D, Eckhardt D, Gerlach D, et al. Downstream processing of Cry4AaCter-induced inclusion bodies containing insect-derived antimicrobial peptides produced in *Escherichia coli*. *Protein Expr Purif* 2019;155:120–9. <https://doi.org/10.1016/j.pep.2018.12.002>. PMID: 30529536.
- [33] Schindler D, Milbredt S, Sperlea T, et al. Design and assembly of DNA sequence libraries for chromosomal insertion in bacteria based on a set of modified MoClo vectors 2016;5:1362–8. 10.1021/acssynbio.6b00089. PMID: 27306697.
- [34] Schreiber C, Müller H, Birrenbach O, et al. A high-throughput expression screening platform to optimize the production of antimicrobial peptides. *Microb Cell Fact* 2017;16:29. <https://doi.org/10.1186/s12934-017-0637-5>. PMID: 28193216.
- [35] Cui W, Xue H, Cheng H, et al. Increasing the amount of phosphoric acid enhances the suitability of Bradford assay for proteomic research.

- Electrophoresis 2019;40:1107–12. <https://doi.org/10.1002/elps.201800430>. PMID: 30570157.
- [36] Zor T, Selinger Z. Linearization of the Bradford protein assay increases its sensitivity: Theoretical and experimental studies. *Anal Biochem* 1996;236:302–8. <https://doi.org/10.1006/abio.1996.0171>. PMID:8660509.
- [37] Trunk T, Khalil HS, Leo JC. Bacterial autoaggregation. *AIMS Microbiol* 2018;4:140–64. <https://doi.org/10.3934/microbiol.2018.1.140>. PMID: [31294207](https://pubmed.ncbi.nlm.nih.gov/31294207/).
- [38] Long CP, Gonzalez JE, Cipolla RM, et al. Metabolism of the fast-growing bacterium *Vibrio natriegens* elucidated by <sup>13</sup>C metabolic flux analysis. *Metab Eng* 2017;44:191–7. <https://doi.org/10.1006/abio.1996.0171>. PMID:8660509.
- [39] Pembrey RS, Marshall KC, Schneider RP. Cell surface analysis techniques: What do cell preparation protocols do to cell surface properties? *Appl Environ Microbiol* 1999;65:2877–94. <https://doi.org/10.1128/aem.65.7.2877-2894.1999>. PMID: 10388679.
- [40] Hoffmann D. Produktion des Insektenmetalloprotease Inhibitoren in *Escherichia coli*: Neuartige Plattformtechnologie für die inclusion body-basierte Produktaufarbeitung. ed. 1. Gießen: Shaker Verlag, 2019. ISBN: 978-3-8440-6677-7. 240 p.
- [41] Costa S, Almeida A, Castro A, et al. Fusion tags for protein solubility, purification, and immunogenicity in *Escherichia coli*: The novel Fh8 system. *Front Microbiol* 2014;5:63. <https://doi.org/10.3389/fmicb.2014.00063>.
- [42] Ki MR, Pack SP. Fusion tags to enhance heterologous protein expression. *Appl Microbiol Biotechnol* 2020;104:2411–25. <https://doi.org/10.1007/s00253-020-10402-8>. PMID: 31993706.
- [43] Kirn TJ, Jude BA, Taylor RK. A colonization factor links *Vibrio cholerae* environmental survival and human infection. *Nature* 2005;438:863–6. <https://doi.org/10.1038/nature04249>. PMID: 16341015.
- [44] Gerlach R, Hensel M. Protein secretion systems and adhesins: The molecular armory of Gram-negative pathogens. *Int J Med Microbiol* 2007;297:401–15. <https://doi.org/10.1016/j.ijmm.2007.03.017>. PMID: 17482513.
- [45] Hou J, Li X, Kaczmarek M, et al. Accelerated CO<sub>2</sub> hydration with thermostable *Sulfurihydrogenibium azorensis* carbonic anhydrase-chitin binding domain fusion protein immobilised on chitin support. *Int J Mol Sci* 2019;20:1494. <https://doi.org/10.3390/ijms20061494>. PMID: 30934614.
- [46] Hashimoto M, Ikegami T, Seino S, et al. Expression and characterization of the chitin-binding domain of chitinase A1 from *Bacillus circulans* WL-12. *J Bacteriol* 2000;182:3045–54. <https://doi.org/10.1128/JB.182.11.3045-3054.2000>. PMID: 10809681.